Experimental Study on Local Compressive Capacity of Reinforced Masonry with Invisible Beams

Fengchi Wang[1,a], Hao Guo[2] and Haiming Hu[3]

[1]*School of Civil Engineering, Shenyang Jianzhu University, Shenyang, China*
[2]*School of Civil Engineering, Shenyang Jianzhu University, Shenyang, China*
[3]*Shenyang Jianzhu University Liberary, Shenyang Jianzhu University, Shenyang, China*
a. cefcwang@sjzu.edu.cn

Keywords: Masonry structure, reinforcement, local compression, invisible beam, steel sheet.

Abstract: Through the study of 8 masonry walls (including contrast specimens) reinforced with invisible beams under concentrated load, an analysis is made of the destruction patterns and load-displacement curves of masonry walls reinforced with invisible beams. The experimental results show that the bearing capacity and crack resistance of reinforced masonry wall with invisible beams under concentrated load is much higher, compared with unreinforced walls. What's more, the wall's ductility and deformability increase significantly. When reaching the ultimate bearing capacity, the transverse and vertical displacements of reinforced specimens improve greatly. The steel sheet has a strong constraint on bulging deformation of the wall, while the lacing bar has a strong supporting capacity on steel sheet, which can delay the steel sheet's entering the yield stage. In addition, the lacing bar can improve the working ability with crack and is useful to enhance the bearing capacity of the specimen.

1. Introduction

In our country, after many years' use and environmental erosion, the existing masonry structures' reliability has decreased remarkably or the structures have been close to the maximum design life. The problem of improving the brittleness and seismic performance of existing masonry structures has become imperative. On environmental protection and green energy conservation grounds, masonry structure reinforcement is accepted as the best choice.

So far, the domestic and foreign researches on the methods of strengthening masonry structures have achieved preferable results and many new types of reinforcement methods have been created. For example, the new methods and technologies[1-3] proposed in China for reinforcing masonry by using carbon fiber, bonded steel technology, GFRP materials, etc. have greatly improved the bearing capacity and seismic performance of masonry. Some developed countries in Europe and America began to pay much early attention to the method of reinforcing masonry structures. A couple of people[4], such as CROCO G, first started to study the use of composite materials to reinforce masonry structures and improve the shear resistance of structures. M.R. Ehsani, H. Saadatm anesh, and A.L-Saidy[5-7] conducted tests under static load on masonry members reinforced with FRP sheets. After reinforcement, ductility and strength of the walls can be improved.

The use of invisible beams to reinforce existing brickwork walls is a new type of reinforcement. After reinforcement, a structure similar to the "template beam" is formed on the upper part of the original wall. This kind of reinforcement method is simple in construction, easy to install and has a good economical result. The bearing capacity and crack resistance of the masonry reinforced with invisible beams are significantly improved, and the ductility and deformability are enhanced, both contributing to the improvement of the seismic performance of the masonry. By means of force analysis of the equivalent "template beam" model specimen, the calculation method of local compressive capacity of the masonry reinforced with invisible beams is proposed, which provides a theoretical basis for engineering practice.

2. Experiment Methodology

2.1. Test Parameter Design and Specimen Production

The specimens are all common burnt clay bricks with strength of MU10. Mortar strength is M10. Steel sheets used for test reinforcement are machined from Q235 steel, with the model of 40mm×4mm. 8.8-grade 8mm high-strength bolts are used as wall-to-pull bolts. The brickwork wall in the test adopts a one-by-one masonry method. The concrete bottom beam is connected to the wall below. The strength grade of the bottom beam concrete is C30, and the specific size of the test piece is shown in Figure 1

(a) Before masonry reinforcement (b) After masonry reinforcement

Figure 1: The effect drawing of masonry.

With reference to the existing reinforcement methods, several key factors are selected to improve the bearing capacity of local compressive masonry wall. These factors include the width of the transverse steel sheet, the preload force of the bolt, and the width of the reinforcing plate at the top of the wall. The specific selection of the test parameters is shown in Table 1.

Table 1: The design parameters of specimens.

Specimen number	Specimen size （mm）	Transverse steel plate spacing	Bolt preload force	Steel plate （mm)
Q-1	1250×1000×240	No	No	No
REQ-1	1250×1000×240	120mm	13.2kN	350×240×20
REQ-2	1250×1000×240	150mm	13.2kN	350×240×20
REQ-3	1250×1000×240	180mm	13.2kN	350×240×20
REQ-4	1250×1000×240	120mm	9.9kN	350×240×20
REQ-5	1250×1000×240	120mm	16.5kN	350×240×20
REQ-6	1250×1000×240	120mm	13.2kN	400×240×20
REQ-7	1250×1000×240	120mm	13.2kN	400×240×20

2.2. Loading System and Measuring Point Layout

The hierarchical loading method[8] was used in the test, and before starting the test loading, the 5%~20% preload of the estimated failure load was applied to the specimen. When formally loading, the load at each stage was10% of the estimated load, and was evenly loaded in 1min ~ 1.5min. After loading for 1min ~ 2min, the load was reduced to 50% of the estimated failure load, and then decreased the load at each stage to 5% of the estimated failure load. When the first crack appears on the wall, the load at each stage was restored to 10% of the estimated failure load. After loading 80% of the estimated failure load, continuous loading was imposed at the original loading speed. When the specimen's crack expanded rapidly and the collected load sharply decreased, the specimen was destroyed and the loading was completed. The test loading device is shown in Figure 2. The displacement meter was installed at the loading point at the top of the specimen, at the center of the bottom beam and on the side of the specimen to observe the vertical displacement at the loading point and the transverse displacement of the specimen during loading. The set position of the displacement meter is shown in Figure 3.

Figure 2: The diagrammatic sketch of loading devic.

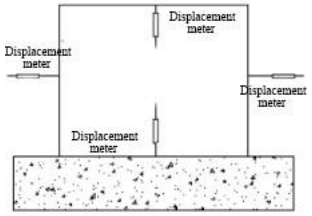

Figure 3: The layout diagram of measuring points.

3. Test Results and Analysis

3.1. Specimen Destruction Pattern

When the unreinforced specimen Q-1 was loaded to 325kN, the first subtle crack appeared near the loading position at the top of the wall, and the second crack appeared at 514kN. When loaded to 564kN, the second crack suddenly widened and extended to the bottom of the wall, showing clearly that the brick was crushed and the wall lost its bearing capacity. When the specimen REQ-1 was loaded to 809kN, the first vertical crack occurred at the third batch of bricks below the loading point and extended downwards to two thirds of the wall. With the load increasing, the cracks continued to extend towards both ends, and many short oblique cracks appeared near the loading point and extended downwards in a divergent manner. As the load continued to increase, the width of the cracks became wider and wider, and the number of cracks increased. Furthermore, the mortar peeled off. At this time, the bearing capacity of the specimen dropped rapidly and then lost, so the specimen was destroyed. The specimens REQ-2 and REQ-3 started to crack when the vertical load was loaded to 809kN, 644kN and 628kN, and the cracks continued to increase and expand as the load enhanced. When the wall came to the ultimate compressive resistance, the bearing capacity dropped promptly to destruction. As to REQ-4 and REQ-5, the first crack appeared when the

vertical load was loaded to 590kN and 550kN respectively. As the load increased, the crack continued to grow and widen. When the capacity reached the peak, it rapidly dropped. And the specimen lost its bearing capacity and was finally destroyed. The specimens REQ-6 and REQ-7 respectively appeared cracks when loaded to 901kN and 680kN. After the continuous loading, the entire wall was seriously deformed, and the distribution of the cracks became significantly larger and destroyed. The destruction patterns of each specimen are shown in Figure 4 (a~h).

(a) Q-1 Destruction Pattern

(b) REQ-1 Destruction Pattern

(c) REQ-2Destruction Pattern

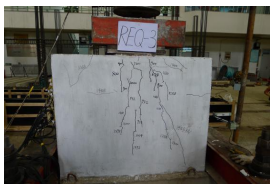

(d) REQ-3 Destruction Pattern

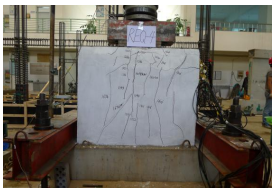

(e) REQ-4Destruction Pattern

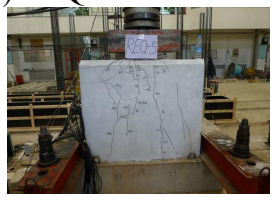

(f) REQ-5 Destruction Pattern

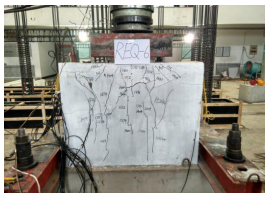

(g) REQ-6 Destruction Pattern

(h) REQ-7 Destruction Pattern

Figure 4: Destruction patterns of specimens.

3.2. Bearing Capacity and Displacement of Specimen

The cracking load and the ultimate load of the unreinforced and reinforced specimens are shown in Table.2. From the detailed comparison of the data in Table.2, it can be seen that, compared with unreinforced wall specimen, the increase in cracking load of wall reinforced with invisible beams is 177.2% at the maximum and 69.2% at the minimum; the increase rate of maximum bearing capacity is 269.7% and the minimum is 89.7%. The local compressive capacity of the specimen reinforced by invisible beam is obviously enhanced.

Table 2: The cracking load and ultimate load of the walls.

Specimen number	Q-1	REQ-1	REQ-2	REQ-3	REQ-4	REQ-5	REQ-6	REQ-7
Cracking load (kN)	325	809	644	628	590	550	901	680
Cracking load increase rate (%)	—	148.9	98.1	93.2	81.5	69.2	177.2	109.2
Ultimate load (kN)	564	1070	1531.7	1455	1674	1396.5	1920	2085.4
Ultimate capacity increase rate (%)	—	89.7	171.6	158	196.8	147.6	240.4	269.7

Table 3 shows the cracking displacements and the ultimate displacements of the unreinforced and reinforced walls. From the data in the table, it can be seen that when the wall reaches the cracking load, the transverse displacement of the specimen REQ-2 is the largest, reaching 0.85mm, with the increase rate of 844%, compared with the unreinforced specimen; the vertical displacement of specimen REQ-1 is the largest, 2.02mm, and the increase rate is 359%. When the wall reaches the ultimate load, the transverse displacement of specimen REQ-7 is the largest, reaching 3.29mm, with the increase rate of 532.7%. The vertical displacement of specimen REQ-1 is the largest, 2.38mm, and the increase rate is 217.3%. When the reinforced specimen comes to the ultimate bearing capacity, the transverse displacement is greatly improved, and the vertical displacement can be increased by five times, which will improve the ductility of the wall to a large extent.

Table 3: The cracking displacement and ultimate displacement of the walls.

Specimen number	Cracking displacement				Ultimate displacement			
	Transverse displacement（mm）	Increase rate (%)	Vertical displacement (mm)	Increase rate (%)	Transverse displacement (mm)	Increase rate (%)	Vertical displacement (mm)	Increase rate (%)
Q-1	0.09	—	0.44	—	0.52	—	0.75	—
REQ-1	0.07	-22	2.02	359	0.34	-34.6	2.38	217.3
REQ-2	0.85	844	0.79	79.5	2.75	428.8	1.31	74.7
REQ-3	0.09	0	0.85	93.1	0.78	50	1.28	70.7
REQ-4	0.03	-66	0.99	125	0.66	26.9	2.36	214.7
REQ-5	0.07	-22	0.54	22.7	0.67	28.8	1.24	65.3
REQ-6	0.09	0	0.66	50	0.72	38.5	1.28	70.7
REQ-7	0.69	-66.7	0.16	-63.6	3.29	532.7	0.58	-22.7

3.3. Load-displacement Curve of Specimen

Figure 5 shows the load-displacement curve of the specimen. As can be seen from Figure.5 (a), comparing the invisible beam specimens of different heights, the load-displacement curve of specimen REQ-1 is similar to that of specimens REQ-2 and REQ-3 at the initial stage of loading. However, when the loading time reaches the middle and late stage, the wall stiffness is significantly lower than the specimens REQ-2 and REQ-3. The load-displacement curves of specimens Q-1, REQ-2, and REQ-3 basically have the same variation trend. The ultimate bearing capacity of Q-1 is quite smaller, while the ultimate bearing capacities of REQ-2 and REQ-3 are greater and closer. Under the same load, the displacement value of specimen REQ-1 is the largest, with the best deformability. Figure.5 (b) indicates the load-displacement curves of specimens with different bolt preload force. In the initial stage of loading, the curve of the specimen REQ-4 basically coincides with that of specimen Q-1. Before the cracking, the initial stiffness of REQ-4 is basically the same as that of Q-1. The initial stiffness of specimen REQ-5 is the smallest. When the load reaches 220kN, the wall stiffness begins to rise greatly and appears an inflection point. The reason is that when there are tiny cracks at the top of the wall, the steel sheet begins to intervene in the work and to be pulled, which makes the rigidity rise dramatically. The curve of REQ-4 increases almost linearly and its stiffness is nearly constant. Figure 5(c) shows the load-displacement curves of the specimens with different plate widths. Under the same load, the displacement of REQ-7 is smaller than that of REQ-6, and REQ-1 and Q-7 are larger. The load-displacement curve of REQ-6

increases almost linearly, and the stiffness remains essentially unchanged. The specimen REQ-7 is in the elastic range at the initial stage of loading, and the curve shows a linear increase. When the load reaches 900kN, the specimen stiffness decreases slightly and then continues to rise. From the load-displacement curve of the specimen, it can be seen that the steel sheet can effectively restrain the bulging deformation of the wall. The bearing capacity and ductility of reinforced wall specimens have been greatly improved, which will help improve the wall energy dissipation capacity under the earthquake.

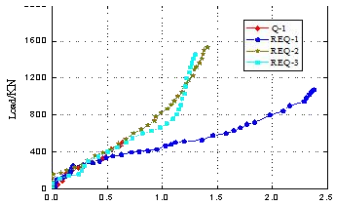

(a) Load-displacement curves of specimens with different invisible beam heights

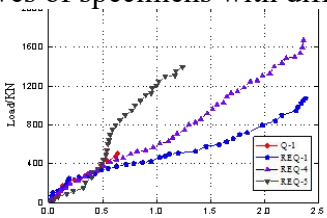

(b)Load-displacement curves of specimens with different bolt preload force

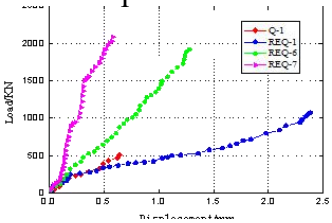

(c) Load-displacement curves of specimens with different plate widths

Figure 5: Load-displacement curves of the specimen.

4. Conclusions

(1) Compared with the unreinforced wall, the masonry wall reinforced with invisible beams under concentrated load has obvious improvement in bearing capacity and crack resistance, and the ductility and deformability of the wall are also significantly improved.

(2)The smaller the spacing of transverse steel sheets, the greater the cracking load; the smaller the bolt preload force, the greater the cracking load; when the plate width is 400 mm, the cracking load is the largest and when the plate width is 450 mm, the bearing capacity is the maximum. The most favorable reinforcement combination is with 150mm transverse steel sheet spacing, 9.9kN bolt preload force, and 450mm plate width.

(3)Compared with the unreinforced specimen, the transverse displacement is greatly increased, and the vertical displacement can increase five times when the reinforced specimen reaches the ultimate bearing capacity. The ductility of the wall is effectively enhanced, which benefits to the seismic resistance of the wall.

(4)The steel sheet has strong restraining capacity for bulging deformation of the wall. The lacing bar has strong supporting ability for transverse steel sheet, which can delay the entering of transverse steel sheet into the yield stage and improve the working ability of the specimen with cracks. It also has a great effect on improving the bearing capacity of the specimen.

Acknowledgments

This work was financially supported by 12th Five-Year Science and Technology Support Program (2012 BAJ11B02) fund.

References

[1] Lu Huifang. Experimental study on reinforcement of masonry walls with holes by carbon fiber cloth[D]. Wuhan: Master thesis of Wuhan University of Technology, 2004:3-15.

[2] Zhang Wei. Finite element analysis and shear capacity of CFRP reinforced masonry [D]. Wuhan: Doctoral dissertation of Wuhan University of Technology, 2007.

[3] Xia Zhangyi. Research on commonly used reinforcement methods for brick masonry walls [D]. Zhejiang: Master thesis of Zhejiang University of Technology, 2013.

[4] Ehsani M. R., Saadatmanesh H., and Velazquez-Dimas J. I. Behavior of retrofitted URM walls under simulated earthquake loading[J]. Journal of Composites for Construction，1999，3（3）：134-142.

[5] Blondet.M, Torrelva.D.and Villa Garcia.G. Adobe in Peru: Tradition research and future, Modem Earth Building[C].2002 International Conference and Fair, Berlin.

[6] Hamilton H. R., Holberg A., Caspersen J. and Dolan C. W. Strengthening concrete masonry with fiber reinforced polymers[C]. Fourth International Symposium on Fiber Reinforced Polymer (FRP) for Reinforced Concrete Structures, Baltimore, Maryland，1999：1103-1115.

[7] Valluzzi M.R., Tinazzi D. And Modena C., Shear behavior of masonry panels strengthened by FRP laminates. Construction and Building Materials，16，2002：409-410.

[8] GB/T2542-2012, Test Method for Brick Wall [S].

[9] Yang Weizhong. Calculation of Local Pressure Bearing Capacity of Beam-end Masonry [J]. Structural Engineer, 2004, 20(4): 42-47.

[10] GB50010-2010, Design Specification for Concrete Structure [S].